J Fluoresc (2017) 27:79–87
DOI 10.1007/s10895-016-1936-7

ORIGINAL ARTICLE

A highly Selective Fluorescent Sensor for Monitoring Cu^{2+} Ion: Synthesis, Characterization and Photophysical Properties

Stephen Opeyemi Aderinto[1] · Yuling Xu[1] · Hongping Peng[1] · Fei Wang[1] · Huilu Wu[1] · Xuyang Fan[1]

Received: 5 July 2016 / Accepted: 12 September 2016 / Published online: 17 September 2016

Abstract A new fluorescent sensor, 4-allylamine-*N*-(*N*-salicylidene)-1,8-naphthalimide (**1**), anchoring a naphthalimide moiety as fluorophore and a Schiff base group as receptor, was synthesized and characterized. The photophysical properties of sensor **1** were conducted in organic solvents of different polarities. Our study revealed that, depending on the solvent polarity, the fluorescence quantum yields varied from 0.59 to 0.89. The fluorescent activity of the sensor was monitored and the sensor was consequently applied for the detection of Cu^{2+} with high selectivity over various metal ions by fluorescence quenching in Tris-HCl (pH = 7.2) buffer/DMF (1:1, *v*/v) solution. From the binding stoichiometry, it was indicated that a 1:1 complex was formed between Cu^{2+} and the sensor **1**. The fluorescence intensity was linear with Cu^{2+} in the concentration range 0.5–5 μM. Moreso, the detection limit was calculated to be 0.32 μM, which is sufficiently low for good sensitivity of Cu^{2+} ion. The binding mode was due to the intramolecular charge transfer (ICT) and the coordination of Cu^{2+} with C = N and hydroxyl oxygen groups of the sensor **1**. The sensor proved effective for Cu^{2+} monitoring in real water samples with recovery rates of 95–112.6 % obtained.

Keywords Naphthalimide · Schiff base · Cu^{2+} · Fluorescent sensor

✉ Huilu Wu
wuhuilu@163.com

[1] School of Chemical and Biological Engineering, Lanzhou Jiaotong University, Lanzhou, Gansu 730070, P. R. China

Introduction

In the recent few decades, much attention has been paid to the science of the design and synthesis of probes for the monitoring of physiologically- and environmentally-relevant metal ions [1–16]. There is no doubt that many metal ions play great and varied roles, however, the ecotoxicological impacts of such metal ions on environmental and biological systems have constituted major challenges for a long time [17]. Among other metal ions, Cu^{2+} ion is an eminent metal ion owing to the indispensable roles it plays by acting as a catalyst and structural cofactor for many metalloenzymes, mitochondrial respiration, iron absorption, free radical scavenging and elastin cross-linking [18–20]. Though regulated amounts of Cu^{2+} ion in human bodies are essential for normal healthy living, however, excess concentrations of Cu^{2+} ion are both toxic and detrimental and can lead to oxidative stress that can in turn be implicated in a number of neuronal cytoplasm neurodegenerative diseases like Wilson's disease, dyslexia, hypoglycemia, Alzheimer's diseaese, Menkes diesease, Parkinson's disease, amyotrophic lateral sclerosis, infant liver damage, and gastrointestinal disease [18, 21–27]. Due to the obvious threatful implications of excess amounts of Cu^{2+} ion, the search for methods for the detection of Cu^{2+} ion has been directed towards the synthesis of chemosensors.

Unlike other conventional analytical techniques, the fluorescence technique is a highly efficient analytical method and has received much research attention due to its relative advantages of high selectivity and sensitivity, intrinsic specificity, real time monitoring and fast response time [28–30]. Owing to their strong absorption and emission in the visible region, high photostability, large Stokes shift and high fluorescence quantum yields, much work is currently in progress in investigating the potent uses of 1,8-naphthalimide derivatives, which are a special class of environmentally sensitive chromophores

[31–39]. This explains the reason why 1,8-naphthalimide derivatives enjoy a wide range of applications as colourants in the polymer industry [40, 41], laser dyes [42, 43], chemosensors [44, 45] and fluorescence probes for biomedical purposes, including fluorescence cell makers [46] and anticancer agents [47].

As such, recently much emphasis has been placed on the applications of Schiff bases in diverse fields including biological medicine, catalytic synthesis, analytical chemistry, anticorrosion, light-induced discoloration, thereby making them one of the most important categories of compounds in biology and chemistry [48].

Herein, we report a Schiff base based fluorescent chemosensor for Cu^{2+} ion, which induces a fluorescence quenching effect upon chelation with the metal ion. The chemosensor displays high and singular selectivity towards Cu^{2+} ion and could thereby distinguish Cu^{2+} when in coexistence with other metal ions under investigation.

Experimental

Materials and General Methods

Unless otherwise stipulated, all chemicals and solvents used for the synthesis were analytical reagent grade and used without further purification. Stock solutions of various metal ions (1 mM) were prepared using the nitrate salt of each metal in double-distilled water. Britton–Robinson (B–R) buffer was prepared with 40 mM acetic acid, boric acid and phosphoric acid. Dilute hydrochloric acid or sodium hydroxide was used for adjusting pH values. Tris-HCl buffer (pH = 7.2) were prepared using bidistilled water.

C, H and N contents were determined using a Carlo Erba 1106 elemental analyzer. The Infrared Radiation (IR) spectra were recorded in the 4000–400 cm^{-1} region with a Nicolet FT-VERTEX 70 spectrometer using KBr pellets. Absorption spectra were scanned using a Lab-Tech UV Bluestar spectrophotometer. Proton nuclear magenetic resonance (^{1}H-NMR) spectra and carbon-13 nuclear magnetic resonance (^{13}C-NMR) spectra were obtained with a Mercury plus 400 MHz NMR spectrometer with trimethyl silane (TMS) as internal standard and DMSO-d_6 as the solvent. Mass spectra (MS) were recorded on a Mass Spectrometer micrOTOF. The corrected excitation and fluorescence spectra were taken on a F97 Pro fluorescence spectrophotometer. A 1 × 1 cm^2 quartz cuvette was used for the spectroscopic analysis. Relative fluorescence quantum yields (Φ_F) were measured using *N*-butyl-4-n-butylamino-naphthalimide (Φ_F = 0.81 in ethanol) [49] as standards. Thin Layer Chromatography (TLC) was performed on silica gel, Fluka F60 254, 20 × 20, 0.2 mm. The melting points were determined by means of a Kofler melting point microscope. The synthetic route to **1** is shown in Scheme 1.

Synthesis of Sensor 1

A suspension of 4-bromo-1,8-naphthalic anhydride (2.77 g,10 mmol) and 80 % hydrazine hydrate (1.25 g, 20 mmol) in 30 mL of ethanol was refluxed with stirring for 4 h [50]. The progress of the reaction was monitored by thin layer chromatography (TLC) using dichloromethane as the eluent. The mixture was cooled and the precipitated solids were filtered, recrystallized from ethanol and dried to afford N-amido-4-bromine-1,8-naphthalimide (**2**) as yellow-brown crystals in 2.49 g (85.6 %) yield. ^{1}HNMR ($CDCl_3$): δ (ppm) = 8.68 (d, 1H, J = 7.2 Hz), 8.60 (d, 1H, J = 8.4 Hz); 8.44 (d, 1H, J = 7.6 Hz); 8.06 (d, 1H, J = 8.06 Hz), 7.87 (t, 1H, J = 7.6 Hz), 5.30 (s, 2H).

To a solution of 1.47 g (5 mmol) of N-amido-4-bromine-1,8-naphthalimide (**2**) in 20 mL 2-methoxyethanol, 1.425 g (15 mmol) of allylamine was added. The resulting mixture was refluxed and stirred for 64 h and then poured into 100 mL of water. The precipitate was collected by filtration, washed with water and dried to give 1.25 g of (92.68 %) of N-amido-4-allylamine-1,8-naphthalimide (**3**). mp:180–182 °C.

Compound **3** (1 g, 3.75 mmol) was dissolved in absolute ethanol (40 mL). An excess of salicylic aldehyde (0.68 g, 5.57 mmol) was added and the mixture was refluxed for 6 h. After the mixture was cooled to room temperature, the precipitate that resulted was filtered, washed with water (3 × 10 mL) and dried to give orange crude product. The crude product was purified by column chromatography on flash silica gel using dichloromethane-acetone (v:v = 5:1, R_f = 0.78) as eluent to give 0.68 g (48.9 %) of the final product (**1**). mp:205–206 °C. Anal. calcd. C 71.15; H 4.61; N 11.31 %; found: C 71.08; H 4.58; N 11.29 %. IR (KBr; ν/cm^{-1}):1701, 1669, 1653, 1582, 1542, 1343, 763. UV-Visible (in DMF, nm): 274, 327, 441. M-S([$C_{22}H_{17}N_3O_3$] + 1) *m/z* = 372.1697. ^{1}H NMR (DMSO-d_6, 400 MHz): δ (ppm) = 8.978(s, 1H), 8.745 (d, 1H, J = 8.4 Hz); 8.50 (d, 1H, J = 7.6 Hz); 8.30 (d, 1H, J = 8.4 Hz); 7.727–7.785 (m, 2H); 7.473–7.511 (m, 1H); 7.011–7.057(m, 2H); 6.768 (d, 1H, J = 8.8 Hz); 5.961–6.003 (m, 1H); 5.196–5.304 (m, 2H); 4.092 (s, 2H). ^{13}C NMR (DMSO-d_6, 400 MHz): δ (ppm) = 169.632, 160.746, 160.175, 158.704, 150.931, 134.700, 134.472, 134.091, 131.264, 130.844, 128.932, 124.596, 122.005, 120.229, 119.719, 117.762, 116.762, 116.335, 107.542, 104.714, 44.933.

Results and Discussion

Molecular Design of Sensor 1 and Synthesis

The design methods of many fluorescent sensors are based on two fundamental principles of photoinduced electron transfer (PET) and internal charge transfer (ICT) [51, 52]. The PET

Scheme 1 Chemical structure and synthetic approach to sensor **1**

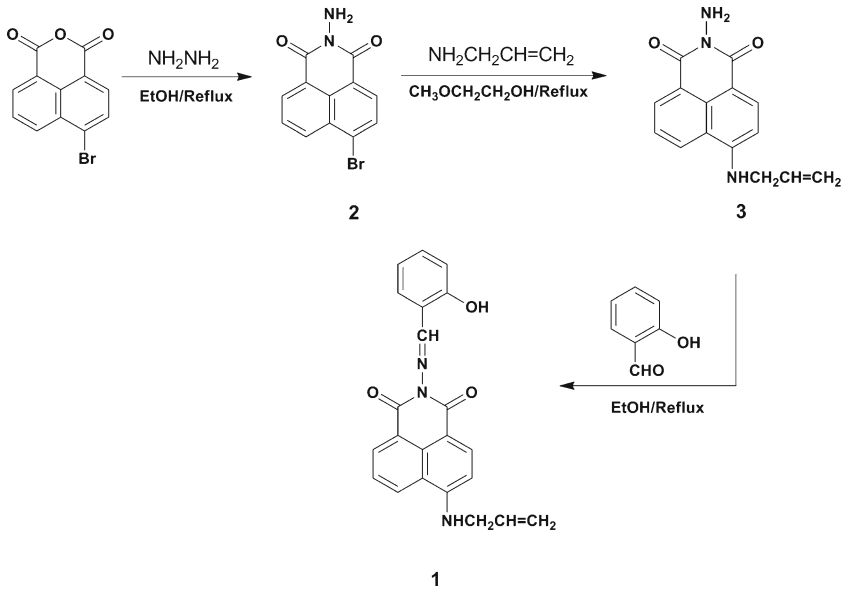

system based on the "fluorophore-spacer-receptor" array stands out as the most widely used method for the design of fluorescent sensors and switches [53, 54]. In the ICT system, there is a direct attachment of the receptor to the electron-donating/withdrawing unit that is conjugated to the fluorophore [51, 52]. During excitation of the system, the fluorophore undergoes donor-acceptor intramolecular charge transfer.

In this current investigation, sensor **1** was designed as a fluorescent probe for the detection of Cu^{2+} ion based on the ICT mechanism. The sensor is based on the "fluorophore-receptor' paradigm in such a way that the fluorophore is directly connected to a receptor sensor with the sensor void of a spacer.

The synthesis of sensor **1** was accomplished via three steps as depicted in Scheme 1. It was fully characterized by elemental analysis, ^{1}H NMR, ^{13}C NMR, UV-vis and IR spectroscopy and mass spectrometry. The spectral and elemental analysis data are all in good agreement with their chemical structures.

Photophysical Characteristics of Sensor 1

As widely known, the photophysical properties of substituted 1,8-naphthalimides are largely dependent on the polarization of their chromophoric systems. Absorption of light in these molecules generates a charge transfer interaction between the substituents at C-4 position and the imide carbonyl groups. We thereby carried out the photophysical characteristics of **1** in acetone, acetonitrile, DMF, tetrahydrofuran and dichloromethane solvents. The absorption (λ_A) and fluorescence (λ_F) maxima, the extinction coefficient (ε), the Stokes shift (υ_A - υ_F), and quantum fluorescence yield (Φ_F) of **1** are presented in Table 1.

As seen from the data in Table 1, compound **1** shows absorption band with maximum range of about 427–441 nm, which is typical for 1,8-naphthalimides substituted in C-4 position with alkylamines. The molar extinction coefficient (ε) falls within the range 10,670–19,390 M^{-1} cm^{-1}, which is higher than 10,000 M^{-1} cm^{-1}, indicating that the absorption spectra band at about 430 nm is attributed to $S_0 \rightarrow S_1$ transition. The respective fluorescence maxima are in the region 502–526 nm.

The photophysical properties of **1** under study is largely influenced by the polarity of the organic solvents, most especially is the quantum fluorescence yield and Stokes shift. The Stokes shift (υ_A - υ_F) reflects the difference in the properties and structure of the fluorophore between the ground state S_0, and the first exited state S_1. We obtained the value of the Stokes shift (cm^{-1}) using the equation (1) [55]:

$$(\upsilon_A - \upsilon_F) = (1/\lambda_A - 1/\lambda_F) \times 10^7 cm^{-1} \quad (1)$$

The Stokes shift values for **1** under investigation are in the region of 3498–3938 cm^{-1}. It is obvious that the value of the Stokes shift depends on the solvent media, with polar solvents

Table 1 Photophysical properties of sensor **1** in organic solvents with different polarity

Organic solution	λ_A(nm)	ε(M^{-1} cm^{-1})	λ_F (nm)	υ_A - υ_F (cm^{-1})	Φ_F
acetone	432	19,390	518	3843	0.59
acetonitrile	433	16,050	522	3938	0.63
DMF	441	18,300	526	3664	0.72
tetrahydrofuran	431	10,670	509	3554	0.81
dichloromethane	427	12,420	502	3498	0.89

yielding larger Stokes shift values than non-polar solvents owing to their more favored hydrogen bond formation or dipole-dipole interactions (Table 1). This observation is in good agreement with investigations on other 1,8-naphthalimide derivatives [56, 57]. The fluorescent quantum yield, Φ_F is another interesting photophysical parameter, which is used to characterize the ability of **1** to emit absorbed light energy. We obtained the value of the fluorescence quantum yield using N-butyl-4-n-butylamino-naphthalimide (Φ_F = 0.81 in ethanol) according to equation (2) [49]:

$$\Phi_F = \Phi_{ref}\left(\frac{S_{sample}}{S_{ref}}\right)\left(\frac{A_{ref}}{A_{sample}}\right)\left(\frac{n_{sample}}{n_{ref}}\right)^2 \quad (2)$$

where Φ_F is the emission quantum yield of the sample, Φ_{ref} is the emission quantum yield of the standard, A_{ref} and A_{sample} represent the absorbance of the standard and sample at the excited wavelength, respectively, while S_{ref} and S_{sample} are the integrated emission band areas of the standard and sample, respectively, and n_{ref} and n_{sample} are the solvent refractive index of the standard and sample, respectively. As expected, the fluorescence quantum yield of **1** in polar solvents is lower than that in non-polar solvents. This is explained on the basis of the photoinduced electron transfer process which is favored in polar solvents with the consequent result of low fluorescence emission [58].

Influence of pH on the Photophysical Properties of Sensor 1

The pH sensing properties of sensor **1** arise from ICT process. After protonation of sensor's imine (C = N) nitrogen, the ICT interaction would be affected and the fluorescence of the system quenched [59]. Therefore, the emission of sensor **1** would experience an "on-state" at neutral media and "switched off" in both acidic and alkaline media. This principle provides the foundation for the effect of pH on the photophysical properties of sensor **1**.

Generally, the sensing behavior of fluorescent sensors is influenced by the protonation or deprotonation of the fluorophore, which in turn affects their sensitivities in the detection of an analyte [60]. The light-harvesting system under this present study was designed as a molecular fluorescent probe for determination of pH changes over a wider pH scale. This is why we chose to investigate the photophysical behavior of **1** in Britton-Robison buffer/dimethyl formamide (1:1) solution at varying pH values. To acquire a great depth of insight, we utilized a wide pH range of 1.81–11.82, adjusted with 0.1 M HCl and/or 0.1 M NaOH, starting from the acidic region. As depicted in Fig. 1, in the 1.81–11.82 pH region, the fluorescence intensity is pH-dependent. The result reveals that the fluorescence intensity of **1** suffered a dramatic decrease when the pH value goes down from 3.78 to 1.81 or goes up from 11.82 to 7.96. However, the fluorescence intensity of **1** did not undergo any significant changes in the range of

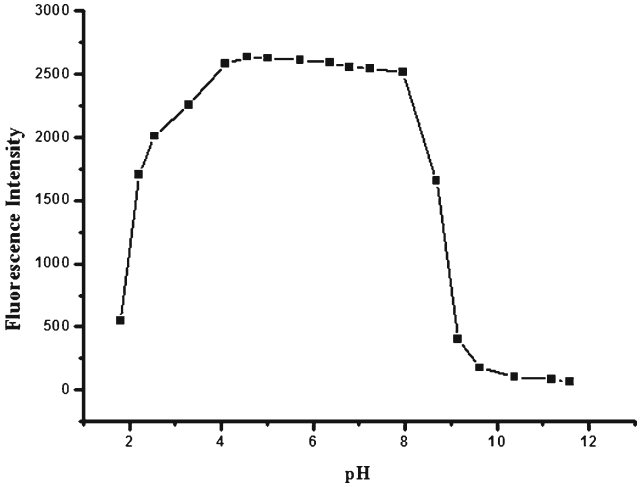

Fig. 1 Photophysical behavior of sensor **1** in Britton-Robison buffer/DMF (1:1) solution at different pH values

pH from 3.78 to 7.96, implying that **1** was actually pH-independent between pH 3.78 to 7.96. In the light of this, we conducted the following experiments in solution at pH 7.2.

Recognition Experiment of Sensor 1 in the Presence of Various Metal Ions

A very crucial feature of any chemosensor is its ability for singular selectivity towards a specific analyte in the presence of competing species. We obtained insights into the fluorescent intensity of **1** as a ligand in the presence of various transition metal cations (Na^+, K^+, Ca^{2+}, Mg^{2+}, Al^{3+}, Pb^{2+}, Fe^{3+}, Ni^{2+}, Zn^{2+}, Cu^{2+}, Hg^{2+}, Ag^+, Co^{2+}, Cr^{3+}, Mn^{2+} or Cd^{2+}, respectively) in Tris-HCl (pH = 7.2) buffer/DMF(1:1,*v*/v) solution. The fluorescence emission spectra were recorded at room temperature with an excitation at 444 nm. In the presence of metal cations in the solution, **1** acts as a ligand during the interaction between the components which is signaled by the changes in the fluorescence intensity. As seen from Fig. 2a, we found that only Cu^{2+} caused a significant fluorescence quenching at 539 nm among the various transition metal ions tested under the same conditions. These results clearly indicate that **1** could be used as a Cu^{2+} selective fluorescent sensor.

Selectivity Study of Sensor 1 for Cu^{2+} Ion over Competitive Metal Ions

To evaluate the affinity of **1** to Cu^{2+}, a competitive binding experiment between Cu^{2+} and other metals to **1** was carried out by using a mixed solution containing Cu^{2+} (10 μM) and each of the other metal cations (Na^+, K^+, Ca^{2+}, Mg^{2+}, Al^{3+}, Pb^{2+}, Fe^{3+}, Ni^{2+}, Zn^{2+}, Hg^{2+}, Ag^+, Co^{2+}, Cr^{3+}, Mn^{2+} or Cd^{2+}) at a concentration of 10 μM in Tris-HCl (pH = 7.2) buffer/DMF(1:1,*v*/v) solution. From the inset Fig. 2b, we can see that there was no obvious discrimination of Cu^{2+} rendered by **1**

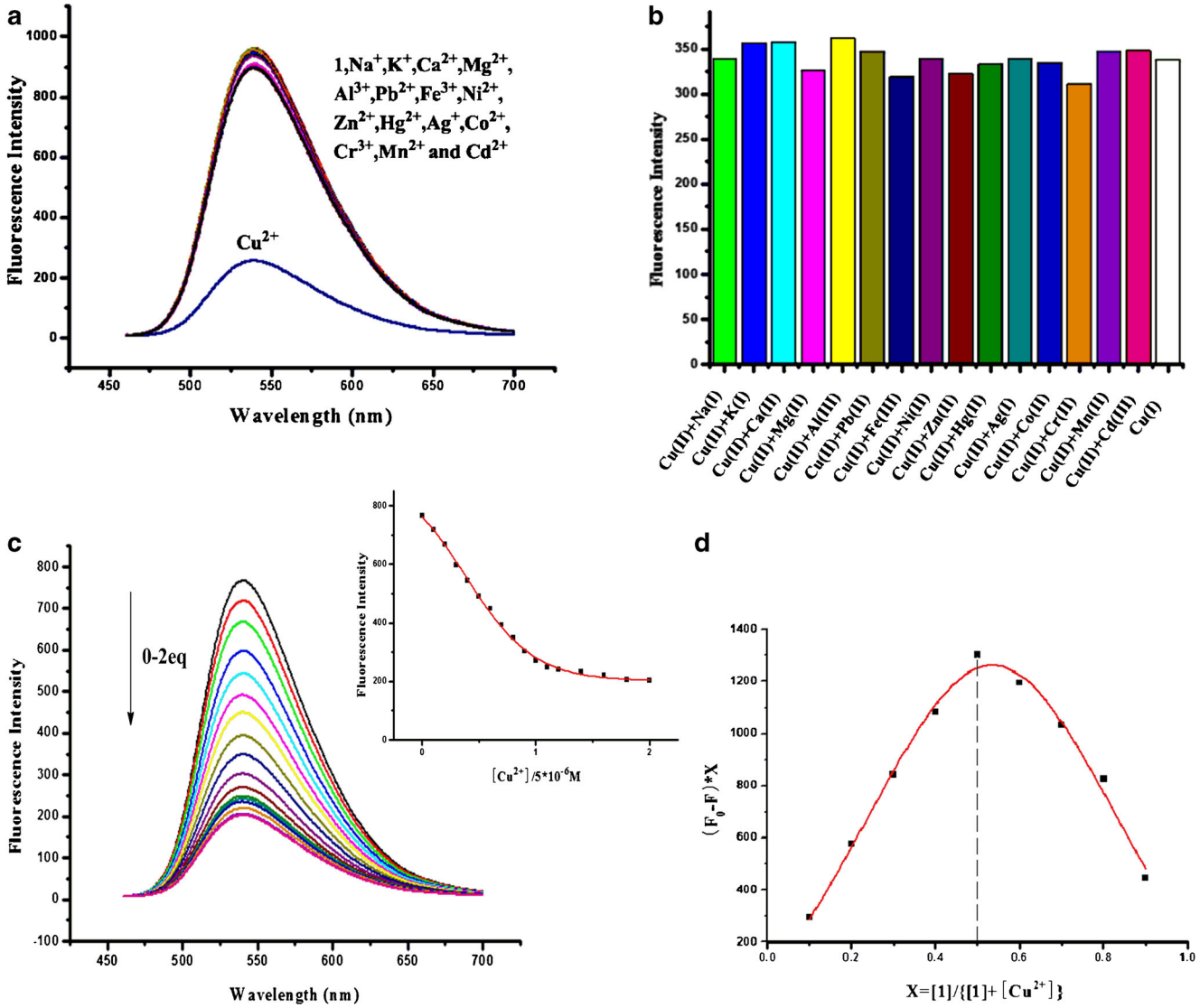

Fig.2 **a** Fluorescence spectra of sensor **1** (5×10^{-6} M) in Tris-HCl (pH = 7.2) buffer/DMF(1:1,*v*/*v*) solution towards Na^+, K^+, Ca^{2+}, Mg^{2+}, Al^{3+}, Pb^{2+}, Fe^{3+}, Ni^{2+}, Zn^{2+}, Cu^{2+}, Hg^{2+}, Ag^+, Co^{2+}, Cr^{3+}, Mn^{2+} or Cd^{2+} (2 eq) with an excitation at 444 nm; **b** Competitive experiments in sensor **1** + Cu^{2+} system with interfering metal ions at 539 nm; **c** Fluorescence titration spectra of sensor **1** with Cu^{2+} (0-2 eq) in Tris-HCl (pH = 7.2) buffer/DMF (1:1, *v*/*v*) solution; **d** Job's plot at 539 nm

even in the presence of competitive metal ions, which implies that compound **1**-Cu^{2+} system was hardly affected by these coexistent ions.

Fluorescence Titration of Sensor 1 in the Presence of Increasing Concentration of Cu^{2+} Ion

In order to gain insight into the binding interaction between **1** with Cu^{2+}, we performed fluorescence titration experiments of **1** with Cu $(NO_3)_2$ in Tris-HCl (pH = 7.2) buffer/DMF(1:1, *v*/*v*) solution. With an increasing concentration of Cu^{2+}, the intensity of the maximum emission at 539 nm suffered a gradual decrease (Fig. 2c). The fluorescence intensity almost reached a minimum when the amount of added Cu^{2+} ion was about 5×10^{-6} M. As more Cu^{2+} was titrated, the fluorescence intensity showed negligible changes. The nonlinear curve fitting of the fluorescence titration gives a 1:1 stoichiometric ratio between compound **1** and Cu^{2+}. Moreover, Job's plot [61], which exhibits a maximum at 0.5 M fraction of Cu^{2+}, indicates that only a 1:1 complex is formed (Fig. 2d).

UV-Vis Titration of Sensor 1 in the Presence of Increasing Concentration of Cu^{2+} Ion

Furthermore, we performed the UV-vis titration experiment of **1** with Cu^{2+} in Tris-HCl (pH = 7.2) buffer/DMF (1:1, v/v) solution. Figure 3 reveals the UV-vis absorption spectra of **1** (5×10^{-6} M) in the presence of various concentrations of Cu^{2+} ion ($0–1 \times 10^{-5}$ M, 0-2 eq) while the inset shows the plot of changes in 326 and 373 nm maxima as a function of increasing

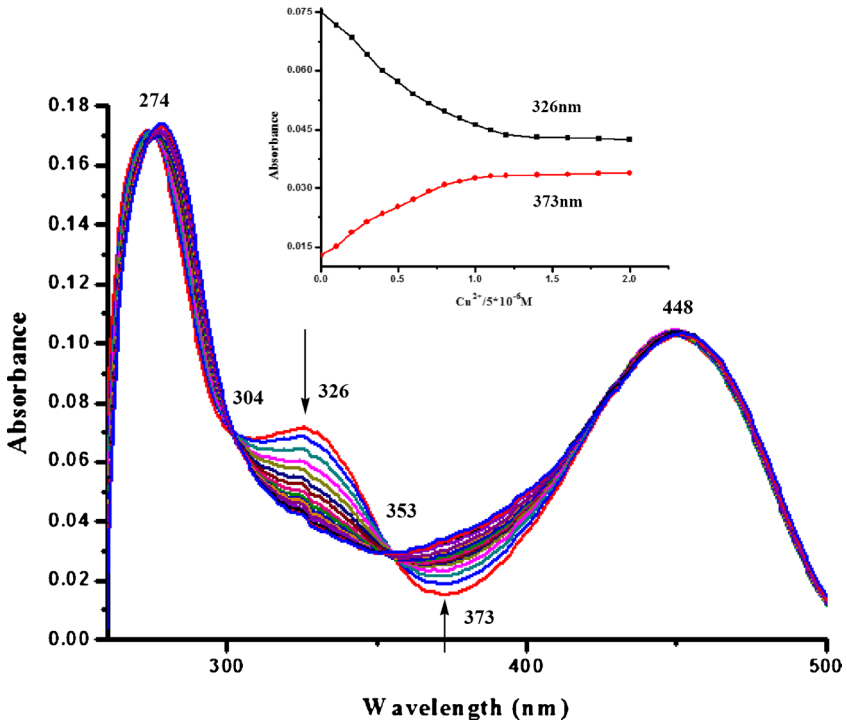

Fig. 3 UV-vis titration of sensor **1** (5×10^{-6} M) in 1×10^{-3} M Tris-HCl (pH = 7.2) buffer/DMF (1:1,*v/v*) solution with increasing amount of Cu^{2+} (0–1×10^{-5} M,0-2 eq) and Absorbance plot of **1** against increasing concentration of Cu^{2+} at λ_{326nm} and λ_{373nm} (inset)

concentrations of Cu^{2+}. The absorbance of **1** at 326 nm gradually decreases with an increasing concentration of Cu^{2+} ion, showing a clear evidence of C = N coordination to Cu^{2+} ion. Owing to the coordination of **1** with Cu^{2+} ion, the absorbance at 373 nm increases with an increasing concentration of Cu^{2+} ion. When the amount of Cu^{2+} ion added was about 5×10^{-6} M, the absorbance of **1** at 326 nm and 373 nm reached a minimum and maximum, respectively. As more Cu^{2+} was titrated, the absorbance showed negligible changes, implying a 1:1 stoichiometry complex was formed. More interesting to note is that two isobestic points appeared at 304 nm and 353 nm. Moreover, the absorption at 274 nm and 448 nm could be assigned to π–π^* transitions of benzene and naphthalene ring, respectively.

Determination of Association Constant and Detection Limit

Based on the fluorescence titration of compound **1** with Cu^{2+}, the association constant has been calculated to be 1.088×10^6 M^{-1} (error limits ≤10 %) by a Benesi-Hildebrand equation [62–64] (Fig. 4).

$$\frac{1}{F-F_0} = \frac{1}{K_a(F_m-F_0)\left[Cu^{2+}\right]^n} + \frac{1}{F_m-F_0} \quad (3)$$

Herein, F is the fluorescence intensity at 539 nm at any given Cu^{2+} concentration, F_0 is the fluorescence intensity at 539 nm in the absence of Cu^{2+}, and F_m is the minimum fluorescence intensity at 539 nm in the presence of Cu^{2+} in solution. The association constant K_a was evaluated graphically by the plot of log $[(F-F_0)/(F_m-F)]$ versus log$[Cu^{2+}]$.

Figure 5 also further confirms the good linearity between the emission at 539 nm and concentrations of Cu^{2+} in the range from 0.5 to 5 μM, indicating that sensor **1** can detect quantitatively relevant concentrations of Cu^{2+}.

We calculated the limit of detection (LOD) based on the definition by IUPAC and the information obtained from the Stern-Volmer plot according to the equation below [65]:

$$C_{DL} = 3\,\sigma/k \quad (4)$$

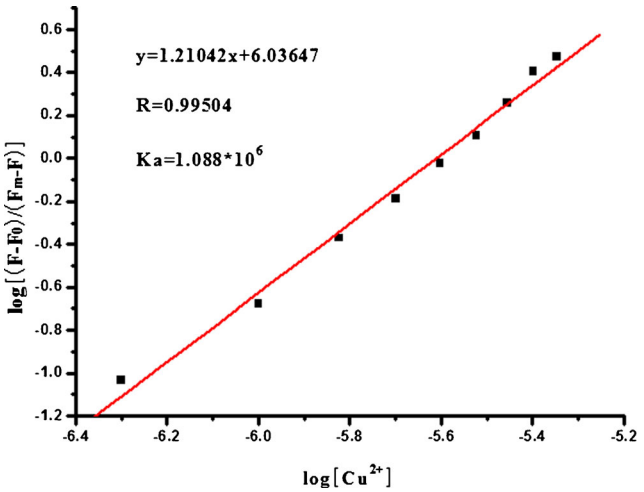

Fig. 4 Benesi-Hildebrand linear analysis plots of sensor **1** at different Cu^{2+} concentration

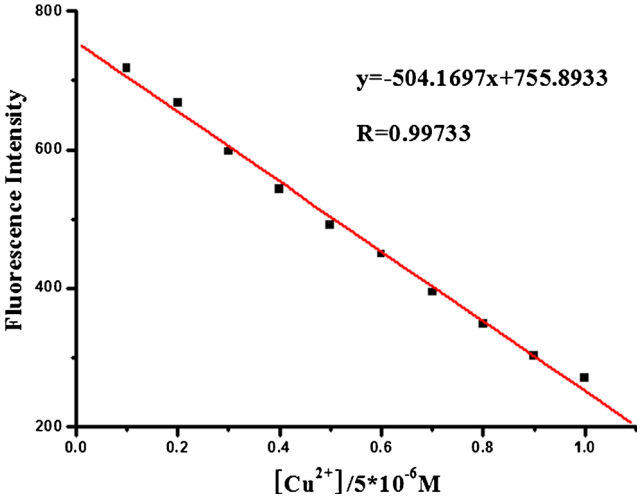

Fig. 5 Curve of fluorescence intensity at 539 nm of sensor **1** (5×10^{-6} M) versus increasing concentrations of Cu^{2+} (0.5–5 μM)

where σ is the standard deviation of the blank solution and k is the slope between F_0/F versus $[Cu^{2+}]$. The value of LOD was obtained to be 0.32 μM, which is far lower than the WHO and U.S. EPA regulated limits of 31.5 μM and 20 μM, respectively [19, 66]. This result substantiates that the proposed sensor **1** could monitor Cu^{2+} ion in sufficiently low concentrations whether in environmental- or biological system.

Effects of Anions on the Sensing Properties of Sensor 1 towards Cu^{2+}

In order to explore the effects of anionic counter-ions on the sensing behavior of **1** to Cu^{2+} ion, fluorescence responses of **1** to sulfate, chloride, bromide, oxalate and nitrate salts of copper were performed in Tris-HCl (pH = 7.2) buffer/DMF(1:1,v/v) solution. As can be seen from Fig.6, there were no

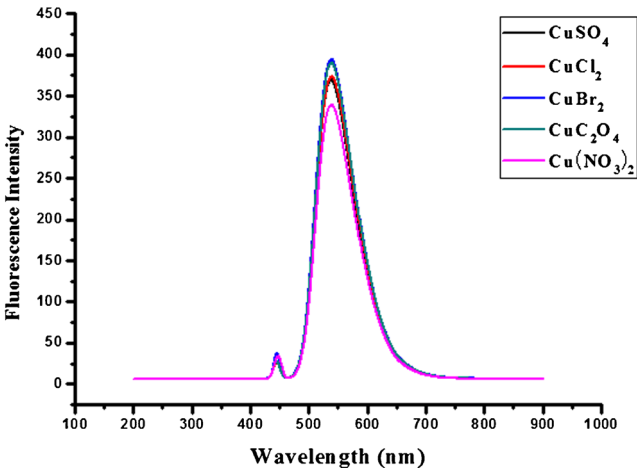

Fig. 6 Fluorescence spectra of sensor **1** (5×10^{-6} M) in Tris-HCl (pH = 7.2) buffer/DMF (1:1,*v*/*v*) solution in the presence of different copper salts (1×10^{-5} M) with an excitation at 444 nm

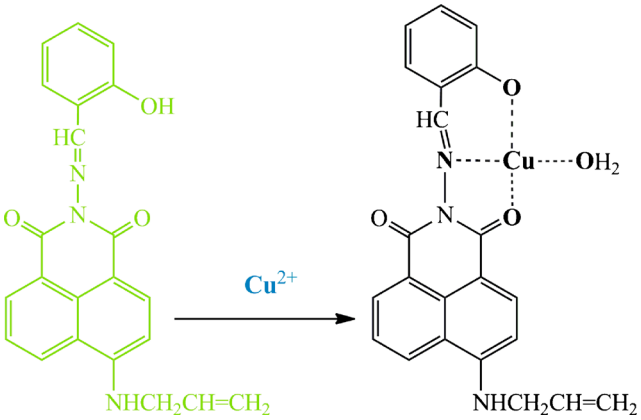

Scheme 2 Proposed binding mode of sensor **1** with Cu^{2+}

noteworthy changes in the fluorescence responses of **1** to $CuSO_4$, $CuCl_2$, $CuBr_2$, CuC_2O_4 and Cu $(NO_3)_2$.

Proposed Binding Mechanism

Based on the results of the absorption titration spectra, fluorescence titration spectra and Job's plot, we hereby propose the binding mode of sensor **1** with Cu^{2+}. As shown in Scheme 2, the mechanism for Cu^{2+} quenching is explained as due to intramolecular charge transfer (ICT) [1, 16, 52]. The chelation between sensor **1** and Cu^{2+} is facilitated by the additional coordination from: (i) the imine group, C = N group, which displays a high level of binding affinity with many transition and post-transition metal ions [67, 68] and (ii) the hydroxyl oxygen group. The sensor **1** was designed in such a way that these two functional groups are positioned in a way that facilitates their proximity to the fluorophore moiety. Upon coordination of Cu^{2+} with sensor **1,** there is a chelation between the metal ion and N of the C = N group and O of the hydroxyl oxygen group, leading to the repression of the fluorescence emission intensity.

Table 2 Results of Cu^{2+} determination in different water samples using sensor **1**

Water sample	Cu^{2+} spiked (μM)	Cu^{2+} recovery, mean S.D. (μM)	Recovery (%)
Yellow river			
	2	2.02 ± 0.02	99
	3	3.04 ± 0.21	102.5
	4	4.54 ± 0.14	98.4
	5	5.32 ± 0.20	108.1
	6	6.15 ± 0.33	111.5
Tap	2	1.99 ± 0.04	95
	3	3.02 ± 0.22	100.3
	4	4.36 ± 0.17	106.8
	5	5.40 ± 0.25	109.1
	6	6.18 ± 0.39	112.6

Application of Sensor 1 for Cu^{2+} Ion Analysis in Water Samples

To evaluate the potential applicability of sensor **1** in real water sample analysis, it was applied for the determination of Cu^{2+} in Yellow River water sample (Yellow River is a popular river in Northwest China that flows through Lanzhou City wherein our school, Lanzhou Jiaotong University is located) and tap water sample (sourced from our school). The pH of all the water samples were suitably adjusted by HEPES aqueous buffer solution (pH = 7.4) and analyzed with sensor **1**. Summarized in Table 2 are the results obtained, which showed excellent recovery and mean S.D. values for all the samples. Obviously, sensor **1** could facilitate the detection Cu^{2+} in real water samples.

Conclusions

In summary, we have designed and synthesized a new fluorescent sensor for the detection of Cu^{2+} ion. The sensor, containing a 1,8-napthalimide moiety and a Schiff base unit, displayed a high selectivity and sensitive towards Cu^{2+} with little interference observed from other coexistent metal ions. According to the results of UV-vis titration, fluorescence titration and Job plot, we determined the binding ratio of sensor-Cu^{2+} complex to be 1:1. The proposed sensor exhibits a linear response towards Cu^{2+} in the concentration range covering from 0.5 to 5 μM with a detection limit of 0.32 μM. These results clearly demonstrate that our proposed sensor could be useful for analysis of Cu^{2+} in environmental samples and even for biological studies.

Acknowledgment The authors appreciate the financial supports from the National Natural Science Foundation of China (Grant No. 21367017), Natural Science Foundation of Gansu Province (Grant No. 1212RJZA037) and Graduate Student Innovation Projects of Lanzhou Jiaotong University, which resulted in this article. Likewise, the first author thanks the Chinese Scholarship Council for awarding him a scholarship opportunity (CSC No. 2014BSZ528) to conduct his Master's program in China.

References

1. de Silva AP, Gunaratne HQN, Gunnlaugsson T, Huxley AJM, McCoy CP, Rademacher JT, Rice TE (1997) Chem Rev 97:1515–1566
2. Gunnlaugsson T, Lee TC, Parkesh R (2003) Org Biomol Chem 1: 3265–3267
3. Misra A, Shahid M, Srivastava P (2012) Sensors Actuators B 169: 327–340
4. Bojinov VB, Panova IP, Simeonov DB, Georgiev NI (2010) J. Photochem. Photobiol A: Chem, 210:89–99
5. Li Q, Guo Y, Shao SJ (2012) *Sensors Actuators B* 171–172:872–877
6. Bargossi C, Fiorini MC, Montalti M, Prodi L, Zaccheroni N (2000) Coord Chem Rev 208:17–32
7. Aragay G, Pons J, Merkoci A (2011) Chem Rev 111(5):3433–3458
8. Quang DT, Kim JS (2010) Chem Rev 110:6280–6301
9. Nolan EM, Lippard SJ (2008) Chem Rev 108(9):3443–3480
10. Hewage HS, Anslyn EV, Am J (2009) *Chem Soc* 131(36):13099–13106
11. Kaur N, Kumar S (2011) Tetrahedron 67(48):9233–9264
12. Kuang GC, Allen JR, Baird MA, Nguyen BT, Zhang L, Morgan Jr TJ, Levenson CW, Davidson MW, Zhu L (2011) Inorg Chem 50(20):10493–10504
13. Dutta M, Das D (2012) Trac-trends Anal Chem 32:113–132
14. Kim HN, Ren WX, Kim JS, Yoon J (2012) Chem Soc Rev 41: 3210–3244
15. Barba-Bon A, Costero AM, Gil S, Parra M, Soto J, Martínez-Máñez R, Sancenón F (2012) Chem Commun 48:3000–3002
16. Valeur B, Leray I (2000) Coord Chem Rev 205(1):3–40
17. Que EL, Domaille DW, Chang CJ (2008) *Chem Rev* 108(5):1517–1549
18. Cho J, Pradhan T, Lee YM, Kim JS, Kim S (2014) Dalton Trans 43: 16178–16182
19. You GR, Park GJ, Lee JJ, Kim C (2015) Dalton Trans 44:9120–9129
20. Tapiero H, Townsend DM, Tew KD (2003) *Biomed Pharmacother* 57(9):386–398
21. Barnham KJ, Masters CL, Bush AI (2004) Nat Rev Drug Discov 3: 205–214
22. Mare S, Penugonda S, Robinson SM, Dohgu S, Banks WA, Ercal N (2007) Peptides 28(7):1424–1432
23. Kim BE, Nevitt T, Thiele DJ (2008) Nat Chem Biol 4:176–185
24. Lee JC, Gray HB, Winkler JR (2008) J Am Chem Soc 130(22): 6898–6899
25. Mokhir A, Kiel A, Herten D-P, Kraemer R (2005) Inorg Chem 44(16):5661–5666
26. Liu J, Lu Y, Am J (2007) *Chem Soc* 129(32):9838–9839
27. Løvstad RA (2004) *Biometals* 17(2):111–113
28. Chen X, Pradhan T, Wang F, Kim JS, Yoon J (2012) *Chem Rev* 112: 1910–1956
29. Fabbrizzi L, Licchelli M, Pallavicini P, Sacchi D, Taglietti A (1996) *Analyst* 121:1763–1768
30. Kramer R (1998) Angew Chem Int Ed 37:772–773
31. Nakaya KI, Funabiki R, Muramatsu H, Shabata K, Matsui M (1999) *Dyes Pigments* 43:235–239
32. Kawai K, Kawabata K, Tojo S, Majima T (2002) Bioorg Med Chem Lett 12:2363–2366
33. Ramachandram B, Saroja G, Sankaran NB, Samanta A (2000) J Phys Chem B 104:11824–11832
34. Das SK, Sahu PK, Kar UP, Rahaman A, Sarkar M, Soni M (2013) J Phys Chem C **117**:14338–14347
35. Huang X, Fang Y, Li X, Xie Y, Zhu W (2011) *Dyes Pigments* 90: 297–303
36. Mohan V, Nijamudheen A, Das SK, Sahu PK, Kar UP, Rahaman A, Sarkar M (2012) Chem Phys Chem 13:3882–3892
37. Wang J, Yang L, Hou C, Cao H (2012) Org Biomol Chem 10:6271–6274
38. Gunnlaugsson T, Kruger P, Jensen P, Pfeffer F, Hussey G (2003) Tetrahedron Lett 44:8909–8913
39. Desislava S, Evgenia VT, Ivo G (2014) J Mol Struct 1071:88–94
40. McGehee MD, Heeger AJ (2000) Adv Mater 12:1655
41. Bojinov V, Grabchev I (2001) *Dyes Pigments* 51:57–61
42. Tian H, He Y, Chang CP (2000) J Mater Chem 10:2049–2055
43. Yang S, Meng F, Tian H, Chen K (2002) Eur Polym J 38:911–919
44. Duke RM, Veale EB, Pfeffer FM, Kruger PE, Gunnlaugsson T (2010) Chem Soc Rev 39:3936–3953
45. Wang B, Anslyn EV (2011) *Chemosensors: Principles, Strategies and Applications*,. John Wiley & Sons, New York, pp. 229–252

46. Qian X, Xiao Y, Xu Y, Guo X, Qian J, Zhu W (2010) Chem Commun 46:6418–6436
47. M. F. Brana and A. Ramos, *Curr. Med. Chem. Anti-cancer Agents.*, 1, 237–255 (2001)
48. Beezer A, Miles R, Shaw E, Willis P (1979) *Experientia* 35:795–796
49. Alexiou MS, Tychopoulos V, Ghorbanian S, Tyman JHP, Brown RG, Brittain PI (1990) J Chem Soc Perkin Trans 2:837–842
50. Chen ZJ, Wang LM, Zou G, Cao XM, Wu Y, Hu PJ (2013) *Spectrochim Acta A* 114:323–329
51. de Silva A, McCaughan B, McKinney B, Querol M (2003) Dalton Trans 10:1902–1913
52. Callan JF, de Silva AP, Magri DC (2005) Tetrahedron 61:8551–8588
53. T. Gunnlaugsson, C. McCoy, R. Morrow, C. Phelan and F. Stomeo, *ARKIVOC VII*, 216–28 (2003).
54. Ramachandram B (2005) *J Fluoresc* 15:71–83
55. Georgiev NI, Bojinov VB (2012) J Lumin 132:2235–2241
56. Sali S, Guittonneau S, Grabchev I (2006) Polym Adv Technol 17: 180–185
57. Grabchev I, Chovelon JM (2008) *Dyes Pigments* 77:1–6
58. Poteau X, Brown AI, Brown RG, Holmes C, Matthew D (2000) *Dyes Pigments* 47:91–105
59. Qian J, Xu Y, Qian X, Wang J (2008) *J Photochem Photobiol A: Chem* 200:402–409
60. Han ZX, Zhang XB, Li Z, Gong YJ, Wu XY, Jin Z, He CM, Jian LX, Zhang J, Shen G-L, Yu R-Q (2010) Anal Chem 82(8):3108–3113
61. Job P (1928) Ann Chim 9:113–203
62. Benesi HA, Hildebrand JH, Am J (1949) *Chem Soc* 71: 2703–2707
63. K. A. Connors, Binding Constants, John Wiley & Sons, New York, 339–343 (1987)
64. Valeur B (2000) *Molecular Fluorescence*. Wiley-VCH, Weinheim, pp. 339–346
65. Joshi BP, Park J, Lee WI, Lee KH (2009) Talanta 78:903–909
66. Jung HS, Kwon PS, Lee JW, Kim JII, Hong CS, Kim JW, Yan S, Lee JY, Lee JH, Joo T, Kim JS (2009) J Am Chem Soc 131(5): 2008–2012
67. Bhardwaj VK, Pannu APS, Singh N, Hundal MS, Hundal G (2008) Tetrahedron 64:5384–5391
68. Pascu SI, Balazs G, Green JC, Green MLH, Vei IC, Warren JE, Windsor C (2010) Inorg Chim Acta 363:1157–1172